Quick extended x-ray absorption fine structure instrument with millisecond time scale, optimized for *in situ* applications

S. Khalid,[1] W. Caliebe,[2] P. Siddons,[1] I. So,[1] B. Clay,[1] T. Lenhard,[1] J. Hanson,[3] Q. Wang,[4] A. I. Frenkel,[4] N. Marinkovic,[5] N. Hould,[5] M. Ginder-Vogel,[5] G. L. Landrot,[5] D. L. Sparks,[5] and A. Ganjoo[6,a)]

[1]*National Synchrotron Light Source (NSLS), Brookhaven National Laboratory, Upton, New York 11973, USA*
[2]*Hasylab, Hamburg, Germany*
[3]*Department of Chemistry, Brookhaven National Laboratory, Upton, New York 11973, USA*
[4]*Department of Physics, Yeshiva University, New York, New York 10016, USA*
[5]*University of Delaware, Newark, Delaware 19716, USA*
[6]*Lehigh University, Bethlehem, Pennsylvania 18015, USA*

(Received 6 July 2009; accepted 28 November 2009; published online 19 January 2010)

In order to learn about *in situ* structural changes in materials at subseconds time scale, we have further refined the techniques of quick extended x-ray absorption fine structure (QEXAFS) and quick x-ray absorption near edge structure (XANES) spectroscopies at beamline X18B at the National Synchrotron Light Source. The channel cut Si (111) monochromator oscillation is driven through a tangential arm at 5 Hz, using a cam, dc motor, pulley, and belt system. The rubber belt between the motor and the cam damps the mechanical noise. EXAFS scan taken in 100 ms is comparable to standard data. The angle and the angular range of the monochromator can be changed to collect a full EXAFS or XANES spectrum in the energy range 4.7–40.0 KeV. The data are recorded in ascending and descending order of energy, on the fly, without any loss of beam time. The QEXAFS mechanical system is outside the vacuum system, and therefore changing the mode of operation from conventional to QEXAFS takes only a few minutes. This instrument allows the acquisition of time resolved data in a variety of systems relevant to electrochemical, photochemical, catalytic, materials, and environmental sciences. © *2010 American Institute of Physics.*
[doi:10.1063/1.3276679]

I. INTRODUCTION

To study the structural changes in the reactions that take place in seconds or subseconds, time resolved x-ray absorption spectroscopy (XAS) was developed in energy dispersive and quick extended x-ray absorption fine structure (QEXAFS) modes. In energy dispersive EXAFS (EDE) one can take the snapshots of the samples at a time scale of few milliseconds.[1–5] EDE can be efficiently used in transmission mode only, and is thus limited to the cases when the samples are concentrated and very uniform in thickness. Detector normalization problems, temporal changes in beam flux, and spatial beam stability can decrease data quality. QEXAFS was developed and applied in solving structure of materials over the past couple of decades by many groups.[6–22] The latest piezodriven technology, developed by Frahm,[8,19] is capable of oscillating the monochromator at high frequencies to collect x-ray absorption near edge structure (XANES) data in 5 ms.

Here we present the description, with multiple examples, of integrated system for time resolved measurements, data collection, and analysis.

II. EXPERIMENT

At the National Synchrotron Light Source (NSLS) located at Brookhaven National Laboratory (BNL), we have incorporated a QEXAFS mode at the bending magnet beamline X18B, while upgrading it to provide energy scanning capability in both conventional and QEXAFS mode.

The NSLS operates at 300 mA beam current and 2.8 GeV electron beam energy. The X18B monochromator is 20 m from the source and receives 1 mrad of horizontal radiation. There are no collimating or focusing mirrors. The 1 eV band pass intensity is in the range of 10^{10} photons/s^{-1}, i.e., enough flux for statistically favorable, millisecond range spectroscopy.

Initial development of QEXAFS was with a relatively slow IK320 optical encoder as part of the VME crate and a 12 bit analog-to-digital (A/D) converter for data recording,[11] which recorded only 1000 data points/s. In this improved version, an IK220 optical encoder and a 16 bit National Instrument A/D converter, model NI 6036E, are used to record 2000 data points/s, and are capable of collecting up to 5000 data points/s.[13] These modules are independent of VME crate and are part of the computer peripheral component interconnect (PCI) slots. The sampling rate is now doubled, and the dynamic range is increased from 12 to 16 bit. The 5000 data points/s limit is due to the encoder readout IK220, which supplies one reading per 100 μS. The same software works

a)Present address: Glass Business and Discovery Center, PPG Industries Inc., Cheswick, Pennsylvania 15024.

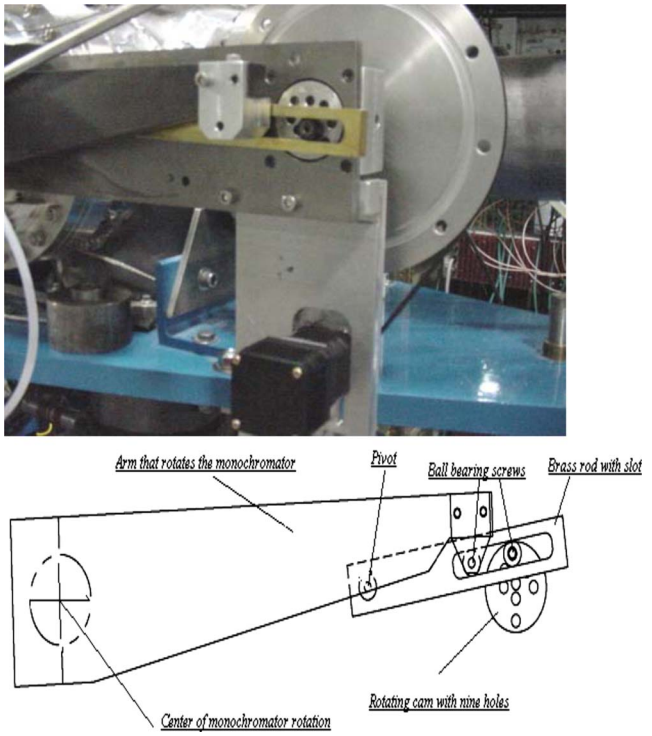

FIG. 1. (Color online) Large wheel attached at the back of the cam with nine holes is driven through a belt and dc motor. The brass rod is attached to the base with a pivot, and to the cam with ball bearing screws. As the wheel turns, the arm oscillates to change the angle of the monochromator.

with the NI PCIe-6251 A/D converter, which is capable of 1 mega-sample/s at 16 bit. Thus, with interpolating the middle values of the optical encoder IK220, a much higher sampling rate can be achieved. Line frequency and its harmonics were observed in the detector output and we found that the high voltage power supply, which was used to bias the ion chambers, was the source of that noise, and it was eliminated by rectifying the power supply.

The white beam slits, upstream of the monochromator, define the energy resolution. The vertical opening of these slits at 17.608 m from the source can be fixed at 1.5, 1.0, 0.5, 0.3, 0.2, or 0.1 mm. The source size of the NSLS x-ray ring is 60 μm and its divergence is 11 μrad. The first crystal of the channel cut Si (111) monochromator is water cooled through gravity flow to avoid vibration and temperature variation. The separation between the first and the second crystal is 3 mm, which minimizes beam walk during a typical scan, eliminating the need to track the sample position with beam energy. The second crystal is bent through a picomotor to reject the higher order harmonics.

The spindle of the monochromator is connected to a 30-cm-long stainless steel arm and, in conventional XAS mode (i.e., using computer automated measurement and control to move the monochromator, stop, settle, and collect data) its end is driven by a motorized micrometer. The spindle is also connected to a Heidenhain optical encoder, which keeps track of the correct position of the monochromator, synchronized with the pulse signal sent to the motor.

In QEXAFS mode, a cam system is used (Fig. 1) to oscillate the monochromator within a defined energy range. The data are collected on the fly, both from low to high and high to low energy ranges. The moving arm, the Heidenhain optical encoder, and the motorized micrometer mechanism are outside the vacuum system and therefore, the procedure of changing the EXAFS setup to QEXAFS and vice versa takes only a few minutes. In this process, the cam, brass rod, wheel, and the dc motor are taken out and replaced by the motorized micrometer, while the optical encoder and the detectors output bypass the IK220 and the A/D converter, respectively.

A. QEXAFS equipment setup

To change the conventional XAS to QEXAFS mode, the motorized linear micrometer is replaced with a cam (Fig. 1) that has nine eccentric holes at different positions, each corresponding to a different angular range. The combination of two pivot positions and nine cam holes gives us an angular range of $\pm 0.22°$ to $\pm 2.25°$. The cam is driven by a dc motor and a belt. A large wheel is attached to the cam, and the shaft of the dc motor is attached to a pulley, which has three different diameters. The wheel to pulley diameter ratios are 10:1, 20:1, and 40:1. By controlling the dc motor speed and wheel to pulley ratio, we can collect EXAFS data from as slow as 15 s/scan to as fast as 100 ms/scan. The belt also helps in damping vibrations transferred from motor to the monochromator.

The cam is on a fixed frame and a brass rectangular rod with a slot in between is attached to the same fixed frame, with a ball bearing pivot on one side and a ball bearing screw attached to the hole of the cam on the other side (Fig. 1). The brass rod can pivot at two different positions. The arm is attached with another sliding ball bearing that goes inside the slot of the brass rod. This whole mechanism moves the arm attached to the monochromator up and down, covering an angular range of the monochromator from 0.44° to 4.5°, depending on the choice of pivot position and the cam hole.

We performed careful noise analysis of the output signal and selected proper filters for high voltage source and Keithley current amplifiers to reduce the noise. The power feedback system for dc motor was also modified to balance the monochromator move when the monochromator arm is moving against the gravity.

B. Data acquisition

The data acquisition system[13] uses a fast computer, EPICS enabled, running Linux operating system. The signals from four x-ray detectors, time, and energy as a function of the optical encoder are read through the National Instrument A/D and IK220 devices, respectively (Fig. 2). The optical encoder has a measuring step size of 0.000 05°, accuracy of ± 1 arc sec, and maximum speed of 5 revolutions/s. The detector output from passivated implanted planar silicon detector or the Lytle detector,[23] if used in fluorescence, goes to Keithley 428 current amplifiers. The amplifiers have their rise time enabled at 1 ms, for 2000 data points/s. This time was optimum for data recording, whereas the smaller or larger rise times resulted in a large shift between the up and down energy spectra.

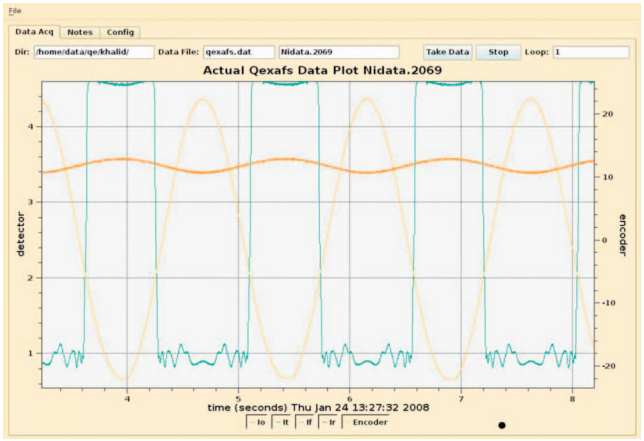

FIG. 2. (Color) The low to high energy and reverse scans are being plotted live. There is also option to plot the sum of all scans at the end of the cycle. In this Ni foil EXAFS, yellow is the relative optical encoder value (covering 0.44° in 0.75 s), and orange (I0) and green (It) are the incident and transmitted flux, respectively.

The graphical user interface of the program controls the motor speed and plots output of all the detectors. The program can acquire data into memory at the above rate. Currently the program options include 30 or 300 s segments, and can run continuously, but require an interruption of 7 and 180 s, respectively. This delay is due to our limitation in resource allocation for the purpose of optimizing the system. The motor speed can be varied continuously from 0.03 to 10 Hz. The data can be plotted as a function of time, when all up and down scans are included, or as a function of encoder value when scans going from the low to high and high to low energy are plotted overlapping each other with the same energy scale along the x-axis.

Offset values are taken with the beam off and the wheel turning with a fixed number of cycles in 30 or 300 s interval, and then the beam is turned on and EXAFS scans are recorded. Offsets should be taken again if the amplifier gains, motor speed, or angular range is changed.

The data are recorded in six columns: time (with μs accuracy), four detector outputs, and the encoder position. A full energy EXAFS scan of Ni foil taken in 120 ms using QEXAFS and compared with a standard EXAFS spectrum taken in 70 min is shown here (Fig. 3). The XANES spec-

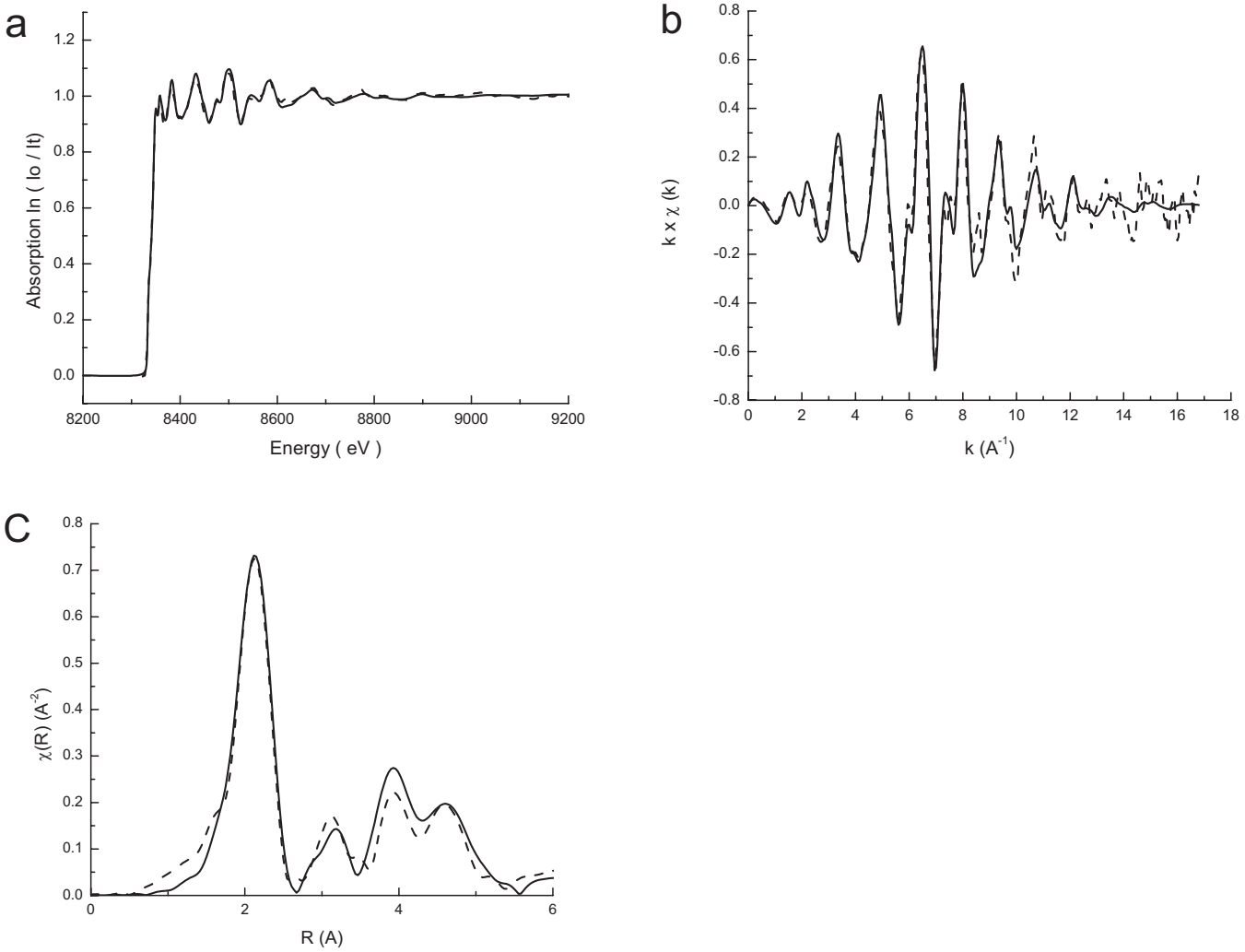

FIG. 3. (a) XAS data of Ni foil at room temperature, (b) Xk as a function of k, and (c) their radial distribution. Solid line is the conventional data taken in 70 min, and dashed line is the QEAXFS data in 120 ms.

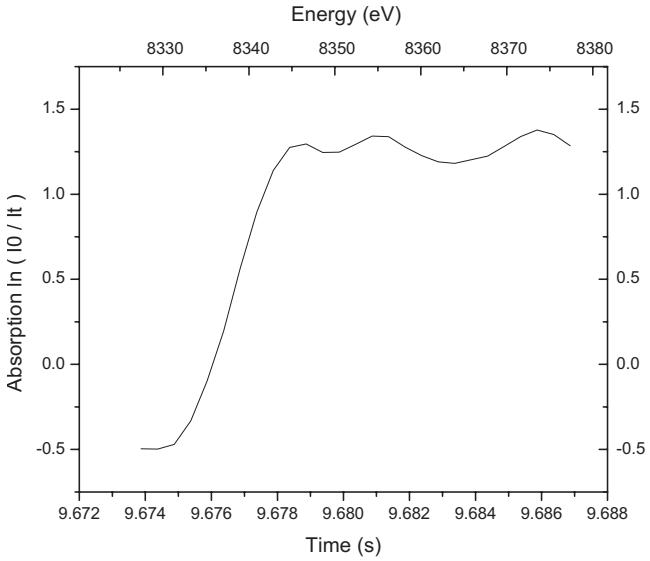

FIG. 4. Ni foil XANES data taken in 13 ms. The data are part of the full QEXAFS scan taken in 120 ms. The edge shoulder is washed out because of fast 1 ms rise time.

trum is recorded here in a few ms, as part of the full XAS scan (Fig. 4) because the shortest angular range of the cam (0.44°, corresponding to about 300 eV at Ni K-edge) did not allow us to take the XANES spectrum only of about 50 eV range at this energy. XANES data at this time scale are useful for most of our applications. Prior to analyzing the EXAFS data with standard programs available, the encoder position needs to be converted to absolute energy.

C. Data conversion and data analysis

The raw data output can be converted to standard EXAFS data format by using home-written FORTRAN programs developed at the chemistry department of BNL, Synchrotron Catalysis Consortium at BNL, and Lehigh University. Additionally, since the output is recorded in a multicolumn text file, individual users can develop specialized data conversion programs. These programs separate low to high and high to low energy scans for a series of segment scans. The program also merges the data and creates data files for linear combination analysis or principal component analysis (PCA). The output data files can be used as input to Athena or WinXAS data analysis programs.[24,25]

Energy calibration is the very first step in the entire procedure. An EXAFS spectrum of a metal foil standard was measured for determination of the conversion from encoder position to energy. The relationship between encoder value and Bragg angle can be described by Eq. (1), in which "intercept" is the unknown

$$\text{Encoder(deg)} = 100^{*}\text{Angle(deg)} + \text{intercept}. \quad (1)$$

As Si(III) is employed for monochromator at this beamline, the Bragg angle can be converted to energy (E) as follows:

$$E(\text{eV}) = 1977.1/\sin\theta$$

$$[2d \sin\theta = n\lambda = hc/E,\ \ hc = 12\,398.6\ \text{eV Å},$$

$$d = 3.135\,56\ \text{Å} = \text{spacing of Si(111)planes}]. \quad (2)$$

The encoder value of the edge position is obtained from the first derivative spectra of the metal foil. The corresponding energy value can be set to the standard value of such metal. Thus, the intercept value in the encoder-angle equation can be found and then can be applied to the experimental data.

QEXAFS data (60 000 data points for every 30 s) are stored in one multicolumn file that contains a multiple traces of spectra, depending on the motor speed. Custom-made programs are then used to crop the files into separate XAS spectrum files.

Data reduction, including bad spectra removal, normalization, and background subtraction, is then applied to the as-collected spectra. Similar spectra obtained in the course of the reaction (i.e., those not changing, within statistical noise) usually are merged. The benefit of such merging is twofold: increasing the signal-to-noise (S/N) ratio and decreasing the number of spectra. In addition, since QEXAFS offers an equal spacing between data points, decided by the motor speed, data rebinning using three regions of the pre-edge, XANES, and EXAFS with some typical step sizes for each region is also applied prior to further operation, which can lead to a better S/N spectra data. However, it is not required if the data quality is sufficiently good for further analysis. Rebinning parameters, especially energy step, need to be reasonable to ensure that data points are not oversampled and are not spaced much denser than the energy resolution of the beamline.

III. APPLICATIONS

In general, there are many applications of QEXAFS in few tens and hundreds of milliseconds time scale, most notably the nucleation and growth of nanoparticles, sulfurization and activation of catalysts, oxidation/reduction, and structural changes in electrode surfaces as a function of charging and discharging.

The majority of the QEXAFS users at X18B beamline applied this method for catalysis, environmental science, optical studies, and electrochemistry.

A. Catalysis

The improvement of catalysts requires knowing the structure of the active catalysts. *In situ* EXAFS and x-ray measurements of Cu doped cerium oxide under water gas reaction conditions shows that the active species is Cu^0 supported on cerium oxide. To understand the transformation to the active catalyst we used QEXAFS to look for short lived intermediates under reducing conditions. Figure 5(a) shows a series of Cu edge QEXAFS scans taken in fluorescence mode from an *in situ* flow cell containing Cu doped cerium oxide. Each scan is an average of many scans taken in a 15 s period. The beginning spectra show the oxidized copper in the cerium oxide and the final spectra show the reduced copper on the surface of the cerium oxide. Principle component analysis of similar data collected at 200 °C in 5%H2/He [Fig. 5(b)], showed that at 1000 s, a reaction intermediate was present.[26,27] There would not have been enough data to observe this intermediate with normal 15 min EXAFS scans.

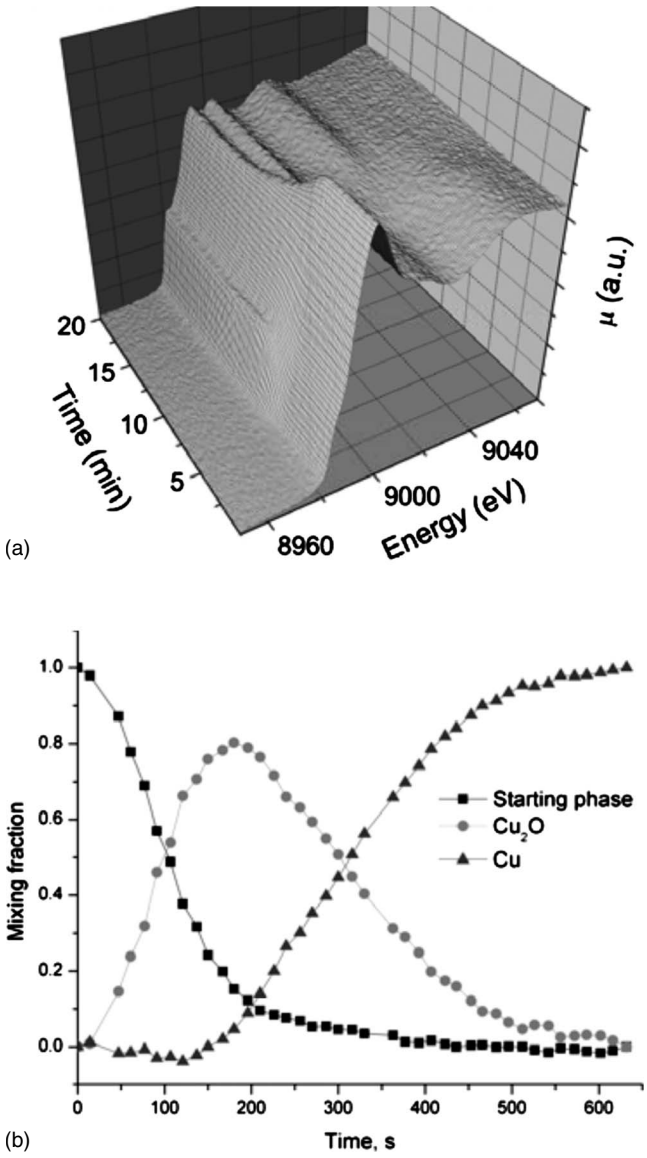

FIG. 5. (a) Time resolved Cu K-edge XANES spectra of Cu doped cerium oxide showing Cu phase transformation during reduction at 275 °C under 5% H_2 in He. (b) Results from PCA analysis of CuO reduction at 275 °C under 5% H_2 in He using three Cu phases [Cu starting phase, Cu_2O, and Cu(0)].

B. Environmental samples

In the environment, chemical reactions at the mineral/water interface occur over a range of temporal scales, ranging from microseconds to years. Many important mineral surface processes (e.g., adsorption, oxidation-reduction, and precipitation) are characterized by a rapid initial reaction on time scales of milliseconds to minutes, in which the significant portion of the reaction process may occur. Knowledge of these initial reaction rates is critical to determining chemical kinetic rate constants and reaction mechanisms, both of which are required to fully understand environmental chemical processes.

For example, the group at Department of Plant and Soil Sciences, Delaware Environmental Institute, University of Delaware has measured the kinetics of As(III) (Ref. 28) oxidation by manganese(IV) with a time resolution of ~1 s (Fig. 6). By using linear combinations to determine the

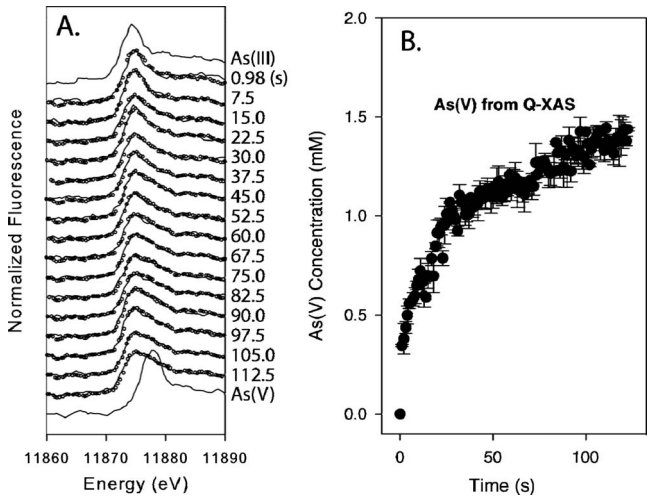

FIG. 6. (a) Data (solid) and linear combination fits (dots) of individual As K-edge XANES spectra used to determine As(III) and As(V) concentrations during the batch reactions. Each spectrum was collected in ~980 ms, with the time (in seconds) next to each spectra indicating the time the last data point of each spectrum was collected. (b) As(V) concentrations determined from QEXAFS reactions.

As(III) and As(V) ratios at each time point, it's possible to determine the oxidation rate during the first 30 s of reaction.

C. Amorphous chalcogenides

In amorphous chalcogenide thin films, the changes in optical properties, such as absorption coefficient, optical band gap, and refractive index are related to changes in structure of the material (Fig. 7). The kinetics and time constant as a function of time for changes in near neighbor distances, Debye–Waller factor, and coordination numbers are best observed by QEXAFS technique. These changes are essential, both from a technological point, for various applications, and from scientific point, for better understanding of the phenomena. The structure and structural changes in amorphous chalcogenides are exploited for various applica-

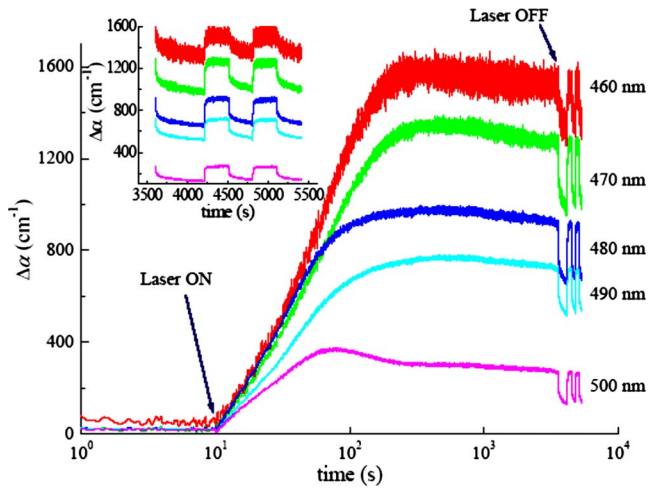

FIG. 7. (Color online) Photoinduced changes in the absorption coefficient as a function of time with LASER ON and OFF. The kinetics of changes correlates with structure changes and with the dynamics of bond breaking and switching. This knowledge can improve its use in various applications.

tions, optical storage devices (e.g., digital video disc), nanotransducers, photoresistors, in the fabrication of infrared waveguides, and other optical components.

The phenomenon of photoinduced structural changes in amorphous chalcogenide films are thoroughly studied, which has both scientific and technological importance.[29,30] Photoinduced changes as a function of time in various optical properties such as the absorption coefficient, optical band gap, and refractive index, which are related to changes in the structure (conversion of homopolar or weak bonds to stronger heteropolar bonds, changing of coordination around chalcogen atoms, etc.) have been investigated by various researchers over the years (Fig. 7). This gives us the information about the time constants and the kinetics of changes.[31] Such *in situ* experiments gave insight into the kinetics of photodarkening, most significantly the total change during illumination consisted of a transient and a metastable part. The transient part decayed once the illumination was switched off, leaving only the metastable part that could be reversed by annealing near the glass transition temperature.[32] We have seen in the past[33,34] the changes in the structure by EXAFS measurements and thus changes in the nearest neighbor distances, the Debye–Waller factor, and coordination number, but these measurements were not done as a function of illumination time because collecting a full spectra takes longer times. Since optical properties are related to the structure of a material and any changes in the optical properties should also induce changes in the structure, the correlation between the kinetics of these two changes and thus the correlation between the time constants is not known. QEXAFS, which gives us the capability to collect a whole scan in milliseconds gives us the ability to get the whole spectra and thus the information about the structural parameters as a function of time. By studying the time variation in the changes in bond distances, the Debye–Waller factor, and the coordination numbers, we are able to estimate the time constants and thus the kinetics of these changes.

This kinetic information is useful as the changes in structure, and thus the optical properties form the basis of using these materials in various applications, namely, fast modulators, optical phase changes memories, nanotransducers, nanoscale photoresistors among others.

IV. CONCLUSIONS

The development of QEXAFS technique at X18B had many applications as illustrated in few of the examples above. The full EXAFS duration, from few tens of milliseconds to few milliseconds for XANES, will find many more applications in the future. The 2000–5000 data points/s produce a large amount of data, and a standardized, simple form of data handling will make it a good general tool for future users. A focused beam available at many beamlines of NSLS and other sources, which will be more intense and brighter at the NSLS-II, will make this tool even more versatile. In the future we are planning to use multielement solid-state detector for very dilute samples, and that will make the system capable of collecting 20–100 channels, instead of a limited four channels at the moment.

ACKNOWLEDGMENTS

Use of the National Synchrotron Light Source, Brookhaven National Laboratory, was supported by the U.S. Department of Energy, Office of Science, Office of Basic Energy Sciences, under Contract No. DE-AC02-98CH10886. Beamline X18B is supported in part by the Synchrotron Catalysis Consortium, U.S. DOE Grant No. DE-FG02-05ER15688. A.I.F and Q.W gratefully acknowledge the support by the U.S. DOE Grant No. DE-FG02-03ER15476.

[1] R. P. Phizackerley, Z. U. Rek, G. B. Stephenson, S. D. Conradson, K. O. Hodgson, T. Matsushita, and H. Oyanagi, J. Appl. Crystallogr. **16**, 220 (1983).
[2] H. Tolentino, F. Baudelet, E. Dartyge, A. Fontaine, A. Lena, and G. Tourillon, Nucl. Instrum. Methods Phys. Res. A **289**, 307 (1990).
[3] P. G. Allen, S. D. Conradson, and J. Penner-Hahn, J. Appl. Crystallogr. **26**, 172 (1993).
[4] G. Aquilanti and S. Pascarelli, J. Phys.: Condens. Matter **17**, 1811 (2005).
[5] O. Mathon, F. Baudelet, J. P. Itie, A. Polian, M. d'Astuto, J. C. Chervin, and S. Pascarelli, Phys. Rev. Lett. **93**, 255503 (2004).
[6] R. Frahm, Nucl. Instrum. Methods Phys. Res. A **270**, 578 (1988).
[7] R. Frahm, Rev. Sci. Instrum. **60**, 2515 (1989).
[8] M. Richwin, R. Zaeper, D. Lutzenkirchen-Hecht, and R. Frahm, J. Synchrotron Radiat. **8**, 354 (2001).
[9] R. Frahm, M. Richwin, and D. Lutzenkirchen-Hecht, Phys. Scr. **T115**, 974 (2005).
[10] R. Frahm, Physica B **158**, 342 (1989).
[11] W. A. Caliebe, I. So, and A. Lenhard, Radiat. Phys. Chem. **75**, 1962 (2006).
[12] R. Frahm and J. Wong, Jpn. J. Appl. Phys., Part 1 **32**, 188 (1993).
[13] I. So, D. P. Siddons, W. A. Caliebe, and S. Khalid, Nucl. Instrum. Methods Phys. Res. A **582**, 190 (2007).
[14] B. S. Clausen, I. Grabaek, G. Steffensen, P. L. Hansen, and H. Topsøe, Catal. Lett. **20**, 23 (1993).
[15] J. Als-Nielsen, G. Grübel, and B. S. Clausen, Nucl. Instrum. Methods Phys. Res. B **97**, 522 (1995).
[16] J. Wong, M. Froba, and R. Frahm, Physica B **208–209**, 249 (1995).
[17] V. A. Sole, C. Gauthier, J. Goulon, and F. Natali, J. Synchrotron Radiat. **6**, 174 (1999).
[18] J. M. Lee, N. E. Sung, J. K. Park, J. G. Yoon, J. H. Kim, M. H. Choi, and K. B. Lee, J. Synchrotron Radiat. **5**, 524 (1998).
[19] D. Lutzenkirchen-Hecht, S. Grundmann, and R. Frahm, J. Synchrotron Radiat. **8**, 6 (2001).
[20] A. J. Dent, Top. Catal. **18**, 27 (2002).
[21] S. G. Fiddy, M. A. Newton, A. J. Dent, J. M. Corker, S. Turin, T. Campbell, J. Evans, A. J. Dent, and G. Salvini, Chem. Commun. (Cambridge) **1999**, 851.
[22] B. S. Clausen, Catal. Today **39**, 293 (1998).
[23] F. W. Lytle, R. B. Greegor, D. R. Sandstrom, E. C. Marques, J. Wong, C. L. Spiro, G. P. Huffman, and F. E. Huggins, Nucl. Instrum. Methods **226**, 542 (1984).
[24] B. Ravel, M. Newville, and J. Athena, Synchrotron Radiat. **12**, 537 (2005).
[25] T. Ressler (WinXAS is a program for x-ray absorption spectroscopy data analysis under MS Windows), J. Synchrotron Radiat. **5**, 118 (1998).
[26] X. Wang, J. A. Rodriguez, J. Hanson, D. Gamarra, A. Martinez-Arias, M. Fernandez-Garcia, and J. Phys, Chem. Br. **110**, 428 (2006).
[27] Q. Wang, J. Hanson, and A. I. Frenkel, J. Chem. Phys. **129**, 234502 (2008).
[28] M. Ginder-Vogel, J. Fischel, L. Landrot, and D. L. Sparks, Proc. Natl. Acad. Sci. U.S.A. **106**, 16124 (2009).
[29] K. Shimakawa, A. Kolobov, and S. R. Elliott, Adv. Phys. **44**, 475 (1995).
[30] A. Ganjoo, N. Yoshida, and K. Shimakawa, *Recent Research Develop-*

ments in Applied Physics, edited by M. Kawasaki, N. Ashgriz, and R. Anthony (Research Signpost, Trivandrum, 1998).
[31] A. Ganjoo and H. Jain, Phys. Rev. B **74**, 024201 (2006).
[32] A. Ganjoo, K. Shimakawa, K. Kitano, and E. A. Davis, J. Non-Cryst. Solids **299–302**, 917 (2002).
[33] G. Chen, H. Jain, M. Vlcek, and A. Ganjoo, Phys. Rev. B **74**, 174203 (2006).
[34] A. Ganjoo, G. Chen, and H. Jain, Phys. Chem. Glasses **47**, 177 (2006).